Impact of Channel Count and PMD on Polarization-Multiplexed QPSK Transmission

C. Xia, W. Schairer, A. Striegler, L. Rapp, M. Kuschnerov, J. F. Pina, and D. van den Borne

***Abstract*—Through graphics-processing-unit-based simulations with different numbers of copropagating channels (1--81), the dependence of the nonlinear threshold on channel count, as well as on the fiber polarization mode dispersion (PMD) coefficient, is investigated for both dispersion-managed and DCM-free 40 and 100 Gb/s coherent-detected polarization-multiplexed quadrature phase-shift keying (CP-QPSK) transmission systems. Different fiber types including standard single-mode fiber (SSMF), large effective area fiber (LEAF), and truewave classic fiber (TWC) are considered and compared. Our investigations show that the required number of simulated copropagating channels to correctly simulate the nonlinear penalty caused by interchannel nonlinearities on CP-QSPK modulation is strongly dependent on the fiber type. The generally used assumption of around ten channels for simulating interchannel nonlinearities is only valid for the SSMF with relative low channel input power. For transmission links consisting of fiber types with low dispersion or high nonlinear coefficients, such as the LEAF or TWC, ten copropagating channels are clearly not sufficient. In dispersion-managed systems with DCMs, the required number of simulated copropagating channels is not only dependent on fiber types and data rates but also strongly on PMD present in the links. Our investigations have indicated that for transmission over fibers with very low PMD (this is the case of most new fibers), ten copropagating channels are not sufficient to correctly characterize the interchannel nonlinearities even for high-dispersion fiber types, such as the SSMF, and hence causes a clear underestimation of the nonlinearity penalty. Finally, synchronized and interleaved CP-QPSK is compared. We show that despite the depolarization effect of PMD, there are still some benefits of using interleaved RZ-CP-QPSK systems.**

***Index Terms*—Coherent detection, digital signal processing (DSP), polarization mode dispersion (PMD), nonlinearity, polarization multiplex, quadrature phase shift keying (QPSK).**

I. Introduction

COHERENT-DETECTED polarization-multiplexed (CP) quadrature phase-shift keying (QPSK) modulation combined with digital signal processing (DSP) has been considered as a very promising technique for next generation high-speed (e.g., 40G and 100G) optical wavelength division multiplexed (WDM) transmission [1]–[6]. Thanks to the fact that group velocity dispersion (GVD) and polarization mode dispersion (PMD) result in linear distortions based on coherent detection, FIR filter-based DSP in the receiver can fully compensate the distortions caused by GVD and PMD. Therefore, CP-QPSK modulated signals mainly suffer from nonlinear transmission impairments, especially interchannel nonlinearities, such as cross-phase modulation (XPM) and cross-polarization modulation (XPolM) [2]–[6].

Computer-based numerical simulations by solving nonlinear Schrödinger equations (NLSE) are a convenient and flexible tool to investigate or predict the system's performance. However, limited by the considerable simulation time required for such simulations, generally only a few copropagating channels [3], [6] (e.g., around ten channels) are used to simulate the nonlinear impairments in a WDM transmission system. The approach to rely on simulations with only few copropagating channels assumes that interchannel nonlinearities in a WDM system are mainly introduced by those neighboring channels that are closely spaced to the channel under test. This assumption is generally valid for WDM transmission over the standard single-mode fiber (SSMF) with large channel spacing, such as 100 or 200 GHz. However, assuming such a limited number of copropagating channels may be insufficient and, hence, cause large estimation errors for a 50 GHz spaced WDM transmission system, in particular, over fiber types with low dispersion and high nonlinearity coefficients. Moreover, compared to single-polarization direct-detection based modulation formats, CP-QPSK suffers not only from XPM but as well from XPolM, which may also cause certain amount of DSP performance degradation. To our knowledge, only a few papers [4], [5] have investigated the channel number impact for CP-QPSK, and with a particular focus on dispersion-managed WDM transmission, where CP-QPSK modulation copropagates with 10 Gb/s OOK channels. Therefore, we investigate and clarify, in this paper, the number of copropagating channels required to characterize interchannel nonlinear impairments in both dispersion-uncompensated and compensated WDM transmission systems. The simulation of a large number of copropagating channels is enabled by graphics processing unit (GPU)-based parallel implementation of the NLSE, which has been demonstrated to speed up the simulations more than 100 times with single-precision fast Fourier transform (FFT) and 40 times with double-precision FFT compared to CPU-based simulations [10], [11]. Double precision has been assumed in this paper due to its negligible errors compared to CPU-based simulations.

PMD is generally considered as an impairment in fiber-optic transmission systems, due to the fact that it results in pulse overlapping and, therefore, pulse distortions. However, the pulse overlap induced through PMD is fully compensated when using

Manuscript received April 04, 2011; revised July 19, 2011; accepted August 21, 2011. Date of publication August 30, 2011; date of current version October 19, 2011.

C. Xia, W. Schairer, A. Striegler, L. Rapp, M. Kuschnerov, and D. van den Borne are with Nokia Siemens Networks, Munich 81541, Germany (e-mail: chunmin.xia@nsn.com; wolfgang.schairer@nsn.com; arne.striegler@nsn.com; lutz.rapp@nsn.com; Maxim.Kuschnerov@nsn.com; d.v.d.borne@ieee.org).

J. F. Pina is with Nokia Siemens Networks, Lisbon 2720-093, Portugal (email: jose.pina@nsn.com).

Color versions of one or more of the figures in this paper are available online at http://ieeexplore.ieee.org.

Digital Object Identifier 10.1109/JLT.2011.2166250

a coherent receiver and DSP for CP-QPSK modulation. Recently, distributed PMD has been found to be beneficial in reducing nonlinear transmission impairments, provided that PMD is fully compensated through DSP in the receiver [6]–[9]. We will make a comprehensive investigation of the dependence of nonlinear tolerance on the number of copropagating channels, as well as the PMD coefficient, in considering different fiber types. Two network scenarios with and without dispersion management are investigated.

Interleaved RZ-CP-QPSK has been demonstrated to result in a higher nonlinear tolerance compared to synchronized CP-QPSK [3], [7]. However, the pulse distortions induced by PMD may reduce the interleaved time alignment between polarizations and, hence, reduce the associated benefit. On the other hand, PMD itself can improve the nonlinear tolerance due to the depolarization it incurs, which can reduce the impact of XPolM. In this paper, we investigate the overall PMD impact in an interleaved RZ-CP-QPSK system, taking into account both the advantages and disadvantages of PMD in CP-QPSK transmission.

The paper is organized as follows. The system setup, simulation assumptions, and fiber parameters are briefly introduced in Section II. Then, the channel-number-dependent nonlinear penalty, as well as PMD impact, for uncompensated links is discussed in Section III. In Section IV, we will discuss the impact of both the number of copropagating channels and the PMD coefficient on the nonlinear penalty for dispersion-compensated links. Finally, the paper is summarized in Section V.

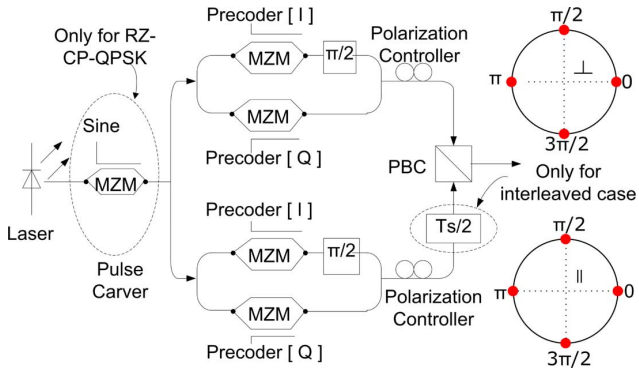

Fig. 1. CP-QPSK transmitter and constellation diagrams.

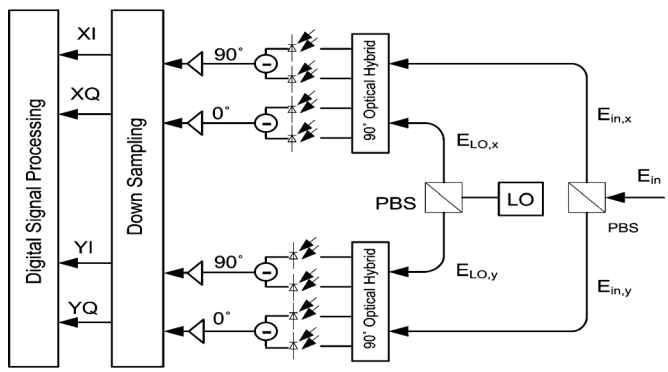

Fig. 2. CP-QPSK receiver.

II. System Model and Assumptions

We assume a 50 GHz spaced WDM transmission system and either 45.8 and 128 Gb/s CP-QPSK modulation (for simplicity called 40G and 100G CP-QPSK). The transmitter is shown in Fig. 1 and consists of two independent QPSK signals, which are generated using two Mach--Zehnder modulators (MZM) and, then, polarization multiplexed using a polarization beam combiner (PBC). An additional MZM is used to generate the RZ-CP-QPSK signal (used in both the 100G and 40G polarization-interleaved case) and one polarization is shifted by half of the symbol period to generate the interleaved CP-QPSK signals. The receiver is shown in Fig. 2, where the received optical field is split into two polarization signals by using a polarization beam splitter (PBS). Then, the two polarization signals are combined with a local oscillator and fed into balanced detectors through a 90° optical hybrid. The four tributary signals are processed further by a sequence of DSP algorithms as shown in Fig. 3. The DSP block contains a frequency-domain equalizer compensating for the major part of the GVD, clock recovery, time-domain equalizer to compensate adaptively for the residual GVD, as well as PMD, carrier recovery, and, finally, a slicer followed by a decoder.

We investigate both dispersion-managed and unmanaged (i.e., DCM-free) transmission systems. We assume a typical optimized dispersion map by optimizing both pre- and inline dispersion in the case of the dispersion-managed transmission system, as shown in Fig. 4. Pre- and inline compensation by using dispersion compensating fiber (DCF) is omitted for DCF-free transmissions. Three representative fibers types, i.e., SSMF, large effective area fiber (LEAF), and truewave classic fiber (TWC) are examined and their parameters are listed in Table I. Without loss of generality, the span length has been assumed to be 80 km and the number of span is set to 20. The PMD in the transmission fiber is emulated by using 800 random waveplates per span. Inline erbium-doped fiber amplifiers are assumed noiseless and noise is only loaded in front of the receiver. We vary the channel number from 1 (i.e., single channel) up to 81 to investigate the impact of different numbers of copropagating channels on the nonlinearity penalty. The center channel (considered as the worst channel from the viewpoint of interchannel nonlinearities) is always examined by calculating the optical-signal-to-noise-ratio (OSNR) penalty based on Monte Carlo simulations. A pseudorandom bit sequence (PRBS) with a length of 1023 is used for the transmitter and channel simulations and in total 131 072 symbols are used to count the resulting BER. For each link simulation, the initial states of polarization (SOPs), bit sequences, timing and phases are randomly initialized, and 30 iterations are carried out to calculate the average, as well as the variance, of the OSNR penalty.

III. Dispersion-Uncompensated Transmission Links

The combination of coherent detection and DSP in the CP-QPSK receiver allows for the full compensation of GVD, which enables DCM-free transmission.

First of all, we investigate the impact of the PMD coefficient on the nonlinearity tolerance. In Fig. 5, we show the OSNR penalty and variance at a BER of 10^{-3} versus PMD coefficient for both 40G and 100G CP-QPSK transmission for 21 copropagating WDM channels over the SSMF. We can see that PMD

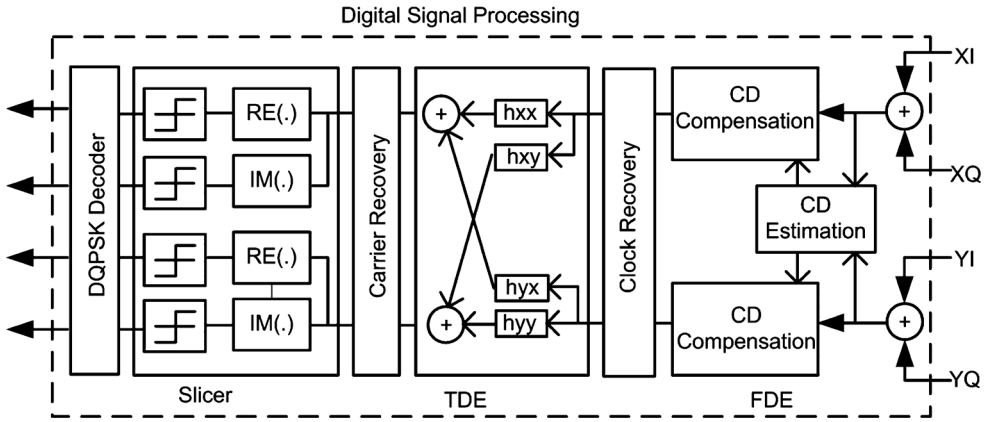

Fig. 3. DSP structure.

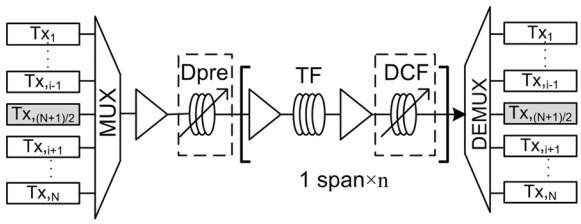

Fig. 4. System setup.

TABLE I

	SSMF	LEAF	TWC	DCF
Dispersion (ps/nm/km)	16.8	4.2	2.8	-170
Slope (ps/ nm^2/km)	0.058	0.086	0.068	Adapted for full compensation
Nonlinearity (1/W/km)	1.14	1.3	2	5
Attenuation (dB/km)	0.21	0.225	0.225	0.5

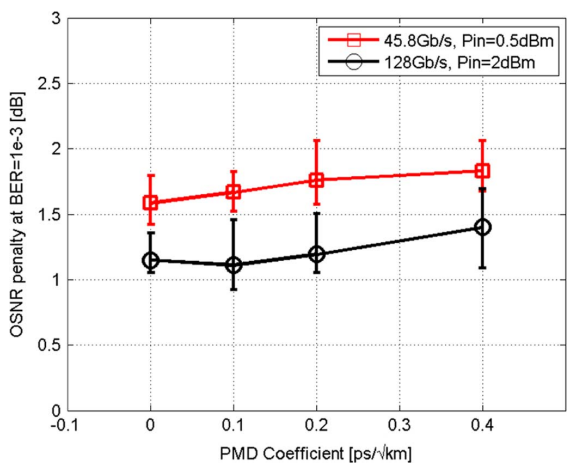

Fig. 5. PMD impact on the nonlinear transmission penalty of 40G CP-QPSK for an uncompensated SSMF transmission link.

impact is quite small and this can be understood from the fact that the PMD depolarization effect is masked by the large accumulated dispersion in a dispersion-uncompensated transmission link. However, as the PMD coefficient is typically less than

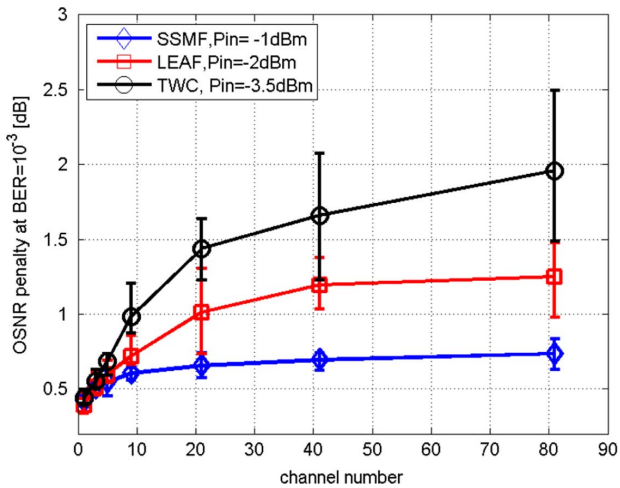

Fig. 6. OSNR penalty versus number of copropagating channels for 40G CP-QPSK transmission over an uncompensated link.

0.1 ps/km$^{1/2}$ for fibers deployed after 1995 [12], [13], and we assume a PMD coefficient of 0.03 ps/km$^{1/2}$ in the following simulations.

We then examine the impact of the number of copropagating channels on the nonlinear tolerance for the three considered fiber types. First of all, relatively low input powers have been assumed, i.e., Pin $= -1, -2$, and -3.5 dBm for SSMF, LEAF, and TWC, respectively. The relative power difference between the different fiber types is chosen based on the expected difference in nonlinear tolerance (determined by both the dispersion and nonlinear coefficients). We see from Fig. 6 that the OSNR penalty increases for a higher number of copropagating channels, as more and more interchannel nonlinear impairments are added to the center channel. However, the SSMF shows that the nonlinear penalty saturates at roughly ten copropagating channels, and a quite small increase in penalty is observed when the number of copropagating channels is further increased from 10 to 80. This confirms that for the SSMF those copropagating channels far away from the center channel have only a negligible contribution to the total nonlinear penalty. In contrast, LEAF and TWC show a much larger increment nonlinear penalty for an increasing number of copropagating channels compared to the SSMF. In particular, TWC that has

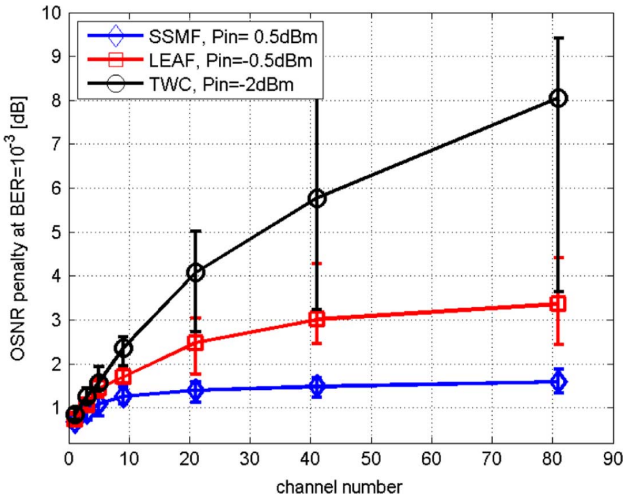

Fig. 7. OSNR penalty versus number of copropagating channels for 40G CP-QPSK transmission over an uncompensated link with increased channel input power.

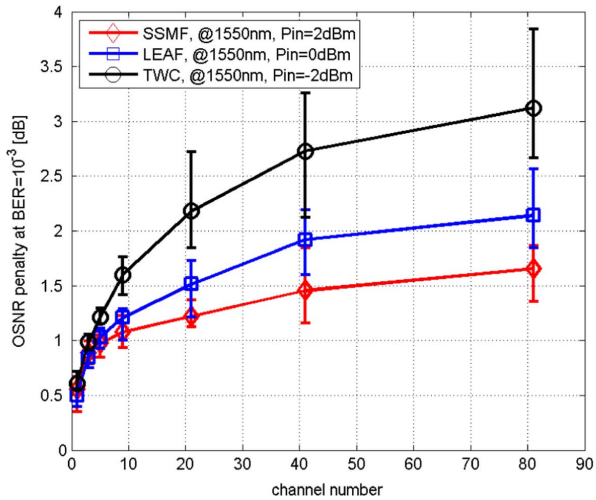

Fig. 8. OSNR penalty versus number of copropagating channels for uncompensated 100G CP-QPSK transmission.

the lowest dispersion and highest nonlinearity coefficient does not show a saturation of the OSNR penalty even at 80 channels and with relatively low input power. The additional nonlinear penalty observed when comparing the simulation results of 80 copropagating channels with those for 40 copropagating channels can only be explained by the large bandwidth of XPolM. In Fig. 7, we show the OSNR penalty versus number of copropagating channels when the channel input power is further increased to -2 dBm. We can see that the increment penalty slope as a function of copropagating channels, as well as the penalty variance, is increased for both LEAF and TWC. However, no significant increase in both penalty slope and variance is observed for the SSMF when comparing $\mathrm{Pin} = -1$ and 0.5 dBm. Comparing the dependence of the nonlinear transmission penalty on the number of copropagating channels for different fiber types, we can draw the conclusion that the required number of copropagating channel to accurately characterize the nonlinear penalty is, approximately, 10, 40, and 80 for SSMF, LEAF, and TWC, respectively.

Fig. 8 shows a similar behaviour for 100G CP-QPSK. At an identical number of copropagating channels, 100G CP-QPSK shows higher nonlinearity tolerance compared to 40G CP-QPSK. This is the result of a lower impact of XPM and XPolM at a higher symbol rate [3]. However, the dependence of the OSNR penalty on the number of copropagating channel is quite similar between 100G and 40G CP-QPSK. This can be explained by the fact that besides XPM, also XPolM is a dominant nonlinear impairment in uncompensated transmission with CP-QPSK, which is not so dependent on the symbol rate [3].

IV. Dispersion-Compensated Transmission Links

Dispersion management has been used in most of the 10G-optimized WDM transmission. In order to upgrade the transmission systems to 40G and/or 100G CP-QPSK, it is necessary to evaluate the performance of CP-QPSK modulation over such dispersion-compensated transmission links.

We assume a residual dispersion per span (RDPS) of 40 ps/nm and optimize the precompensation for each fiber type separately.

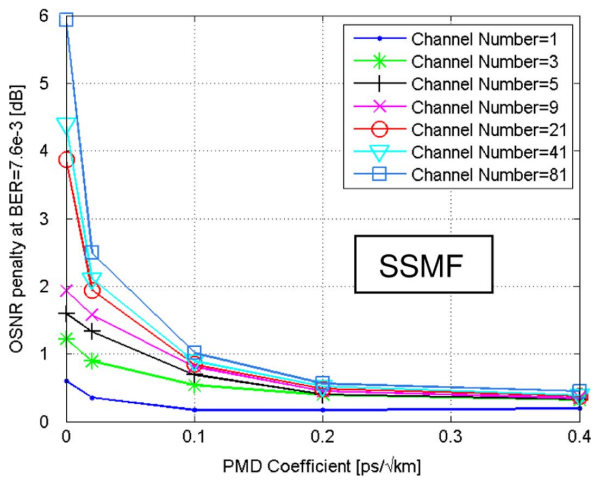

Fig. 9. OSNR penalty versus PMD coefficient for different numbers of channels over SSMF with $\mathrm{Pin} = -1$ dBm.

Note that 0 ps/nm of the RDPS (i.e., fully compensated case) leads to generally the worst nonlinear tolerance, and a higher RDPS value generally improves the transmission performance. We have assumed a 40 ps/nm RDPS in the following simulations in order to approach the dispersion map as it is deployed in most 10G optimized links.

Previous work [6]–[9] has demonstrated that the depolarization effect of PMD improves the nonlinearity tolerance by reducing XPolM in dispersion-compensated CP-QPSK transmission systems. Therefore, in contrast to the dispersion-uncompensated transmission discussed in Section III, we will now investigate OSNR penalty versus both number of copropagating channels and PMD coefficient for dispersion-managed CP-QPSK systems.

Fig. 9 shows the mean OSNR penalty at a BER of 7.6×10^{-3} (the 7.6×10^{-3} target BER is used here instead of 1×10^{-3} due to the error floor that appears around 1×10^{-3} for some cases with 81 channels). First of all, we can observe that the OSNR penalty is reduced with an increasing PMD coefficient at a fixed number of copropagating channels. A 0.2 $\mathrm{ps/km^{1/2}}$

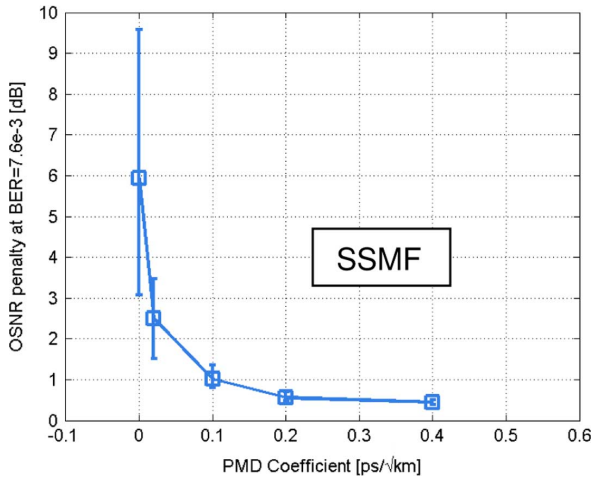

Fig. 10. OSNR penalty and its variance versus the PMD coefficient for dispersion-compensated 40G CP-QPSK transmission over the SSMF with 81 channels and $\mathrm{Pin} = -1$ dBm.

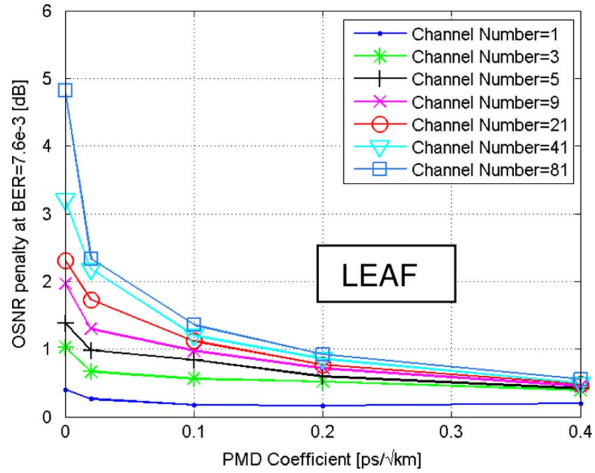

Fig. 11. OSNR penalty versus PMD coefficient for different numbers of channels over LEAF with $\mathrm{Pin} = -2$ dBm.

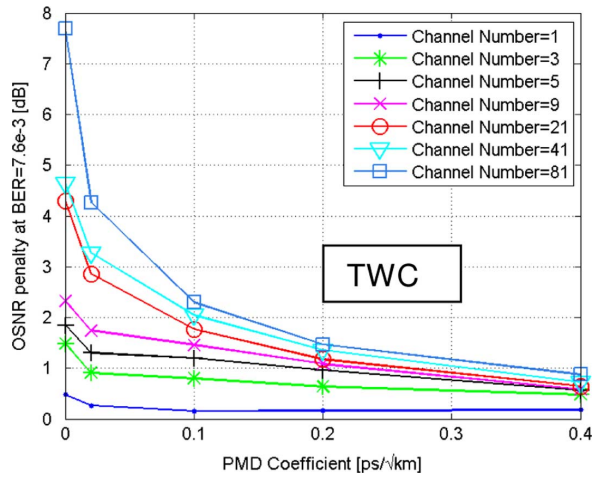

Fig. 12. OSNR penalty versus PMD coefficient for different numbers of channels over TWC with $\mathrm{Pin} = -3$ dBm.

PMD coefficient seems to be enough to reduce the XPolM impact and achieve near-to-optimum transmission performance. As evident from Fig. 9, even a small PMD significant reduces the nonlinear penalty. Moreover, the performance improvement due to PMD is higher for a higher number of channels since XPolM increases for high channels. In Fig. 10, we show separately the OSNR penalty and variance versus PMD coefficient for the case of 81 copropagating channels. We see that more than 5 dB nonlinearity tolerance improvement can be achieved with a high enough PMD coefficient in comparison to the case without PMD. Moreover, the higher the PMD coefficient, the smaller the variance is. This confirmed that random PMD depolarizes CP-QPSK signals, averages out XPolM effect, and thus reduces the nonlinear penalty, as well as its variance.

Secondly, we can observe that for a fixed PMD coefficient, the OSNR penalty increases with an increasing number of copropagating channels. However, in contrast to the dispersion-unmanaged transmission, the OSNR penalty dependence on the channel number is strongly dependent on the PMD coefficient. With no or only small PMD (less than 0.1 ps/$\mathrm{km}^{1/2}$), no saturation behavior is observed and there is about a 1.5 dB difference between 40 and 80 copropagating channels. However, the impact of the number of copropagating channels becomes smaller with increasing PMD. For example, 81 channels results in similar penalty to only three channels with a PMD coefficient of 0.4 ps/$\mathrm{km}^{1/2}$.

Similar simulations have been carried out for LEAF and TWC, and the results are shown in Figs. 11 and 12, respectively. A similar dependence of OSNR penalty on either the number of copropagating channels or the PMD coefficient is observed. The most important difference between the three fiber types is the PMD coefficient required to reach penalty saturation. For example, a 0.5 dB improvement is observed for TWC when the PMD coefficient is increased from 0.2 ps/$\mathrm{km}^{1/2}$ compared to 0.4 ps/$\mathrm{km}^{1/2}$, while only a negligible improvement is observed for the SSMF. This observation is related to the fact that both XPM and XPolM effects are related to fiber parameters including dispersion and nonlinear coefficients. Namely, the lower the dispersion coefficient and the higher the nonlinear coefficient are, the higher XPM and XPolM effects will be.

Similar simulations have been carried out for 100G CP-QPSK, and the results for SSMF are shown in Fig. 13. The nonlinear tolerance improvement due to PMD is expected to be smaller for 100G than 40G.

In order to better understand the impact of PMD on CP-QPSK transmission, we show the SOPs of a sampled signal (i.e., symbols) on the Poincaré sphere. Fig. 14 shows 40G CP-QPSK signals distorted by nonlinear impairments in a LEAF transmission link with a channel input power $\mathrm{Pin} = -2$ dBm and for different PMD coefficients. Note that GVD has been fully compensated and distortions are only caused by nonlinear impairments and PMD.

Fig. 14(a) shows the back-to-back (B2B) 40G CP-QPSK signal distribution on the Poincaré sphere, where the four SOP states (S2, $-$S2, S3 and $-$S3) can be clearly observed. The nonlinear impairments scatter out the points on the Poincaré sphere, as can be observed from the SOP distribution is shown in Fig. 14(b), where the PMD coefficient is assumed to be zero. When the PMD coefficient is increased to 0.02 ps/$\mathrm{km}^{1/2}$km,

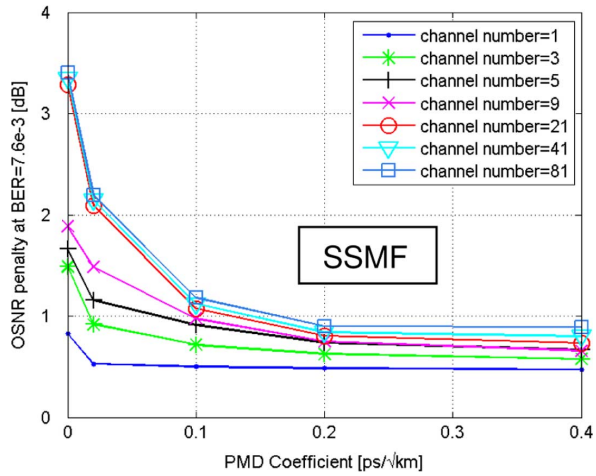

Fig. 13. OSNR penalty versus PMD coefficient with different channel numbers for 100G CP-QPSK transmitted over a dispersion-compensated SSMF link with $\mathrm{Pin} = 1$ dBm.

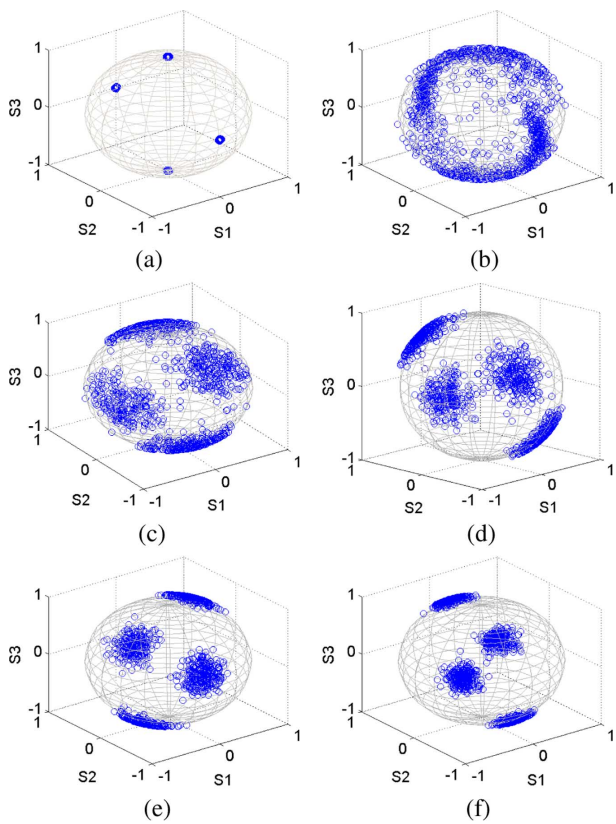

Fig. 14. SOPs on the Poincaré sphere with different PMD coefficients for 40G CP-QPSK transmitted over a dispersion-compensated LEAF link with 81 channels and $\mathrm{Pin} = -2$ dBm. PMD coefficients (ps/km$^{1/2}$) are (a) back-to-back, (b) 0, (c) 0.02, (d) 0.1, (e) 0.2, and (f) 0.4.

as shown in Fig. 14(c), the four SOPs have been roughly separated. This can be attributed to the depolarization effect of PMD, which reduces the impact of XPolM. When the PMD coefficient is further increased to 0.2 ps/km$^{1/2}$ [see Fig. 14(e)] or even 0.4 ps/km$^{1/2}$ [see Fig. 14(f)], the spread of SOPs become smaller and smaller. Note that the mean DGD of 16 ps (with the PMD coefficient of 0.4 ps/km$^{1/2}$) has not been compensated by DSP yet. However, the DGD itself causes relatively small distortions compared to the nonlinear impairments.

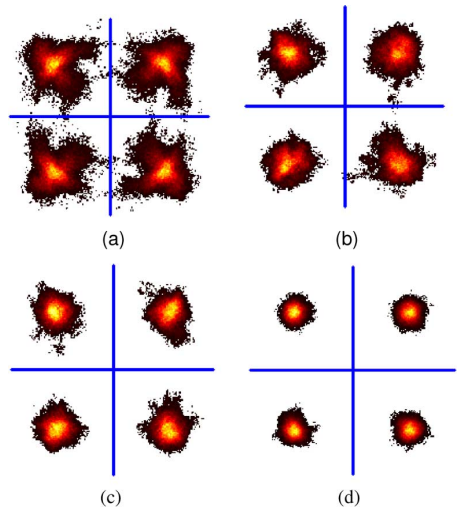

Fig. 15. Constellation diagrams with different PMD coefficients for 40G CP-QPSK transmission over a dispersion-compensated LEAF link with 81 channels and $\mathrm{Pin} = -2$ dBm. PMD coefficients (ps/km$^{1/2}$) are (a) 0, (b) 0.02, (c) 0.1, and (d) 0.4.

In Fig. 15, we show the corresponding constellation diagrams (only one polarization is shown here). In order to clearly see the impact of PMD, no noise has been added to the signals. Fig. 15(a) shows the signal constellation with no PMD. We can observe large variances for all the four symbols caused by XPolM-induced nonlinearities. Moreover, the non-Gaussian shapes of the constellation indicates a strong penalty variance due to XPolM. When the PMD coefficient is increased, the variance is reduced and the shape approaches a Gaussian distribution. This is again due to the average effect brought by PMD-induced depolarization. When PMD is increased to be 0.4 ps/km$^{1/2}$, as shown in Fig. 15(d), the four symbols of CP-QPSK signals are clearly visible with near noise-like Gaussian-distributed samples.

Fig. 16 shows the degree of polarization (DOP) of the CP-QPSK signal as a function of the PMD coefficient. The center CP-QPSK channel has been replaced by a single-polarization QPSK signal in order to determine the DOP. We can observe that the DOP increases by increasing the PMD coefficient, which is consistent with the aforementioned analysis.

So far, we have focused the discussion on synchronized CP-QPSK transmission. It has been previously shown that interleaved CP-QPSK of RZ pulse shaping with one polarization signal delayed by half the symbol rate achieves a higher nonlinearity tolerance compared to synchronized CP-QPSK [3]. A higher PMD coefficient has been previously shown to improve the nonlinear tolerance in synchronized CP-QPSK systems on one hand, but it will also reduce the effectiveness of the time alignment between the two interleaved polarizations, which may reduce the benefit brought by pulse interleaving.

We take a 40G CP-QPSK signal transmitted over the SSMF as a typical example to investigate the impact of different numbers of copropagating channels, as well as the PMD impact, for interleaved RZ-CP-QPSK transmission (see Fig. 17). Note that the channel input power has been assumed to be as high as 4 dBm (i.e., 5 dB higher than synchronized case shown in Fig. 9) since interleaved RZ-CP-QPSK has much higher nonlinear threshold

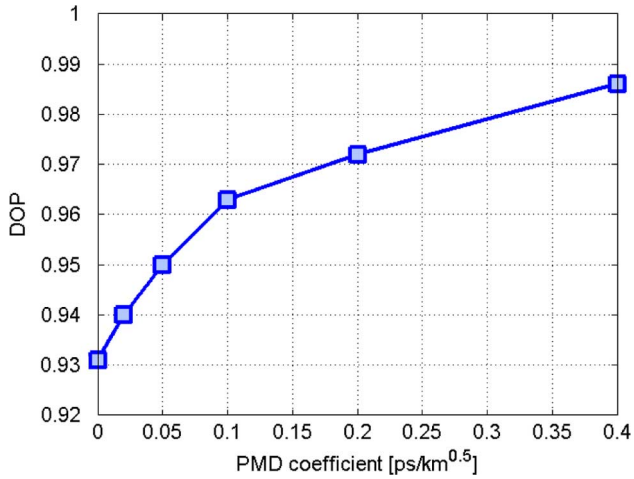

Fig. 16. DOP versus PMD coefficient for 40G CP-QPSK transmitted over a dispersion-compensated LEAF link with 81 channels and a channel input power $\mathrm{Pin} = -2$ dBm.

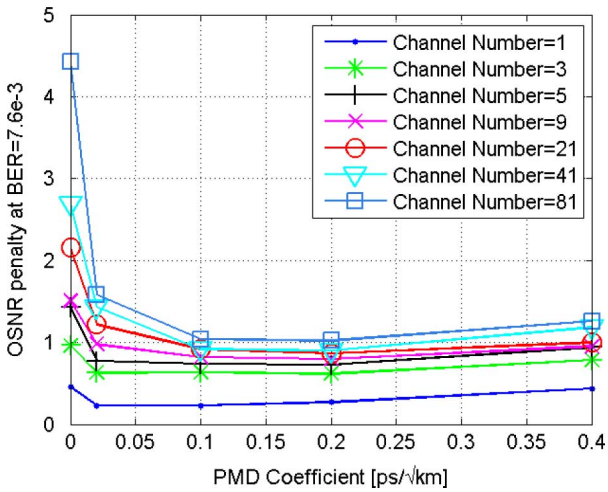

Fig. 17. OSNR penalty versus PMD coefficient for different numbers of co-propagating channels for a 40G interleaved RZ-CP-QPSK signal transmitted over a dispersion-compensated SSMF link with $\mathrm{Pin} = 4$ dBm.

when compared to synchronized RZ-CP-QPSK. We see from Fig. 17 that PMD still reduces the nonlinearity penalty despite that PMD itself breaks out the perfect time alignment. Compared to synchronized CP-QPSK, the benefit brought by PMD in the nonlinear regime is smaller for interleaved RZ-CP-QPSK as the data-dependent XPolM effect is significantly reduced by the pulse interleaving.

V. Conclusion

Using a GPU-based parallel implementation of the split-step Fourier method, we have investigated the impact of the number of copropagating WDM channels, as well as the PMD coefficient, on the nonlinear penalty for 40G and 100G CP-QPSK.

For dispersion-uncompensated transmission, our study has indicated that the general assumption of using only few channels (e.g., approximately 10) in simulations is only a valid approach for the SSMF. It clearly underestimates the penalty for low-dispersion fiber types, such as LEAF and TWC. This conclusion holds for both 40G and 100G CP-QPSK and is, therefore, not strongly dependent on the symbol rate.

For dispersion-managed transmission, the nonlinear penalty is not only dependent on the number of copropagating channels but depends also strongly on the PMD coefficient. The nonlinearity tolerance is improved by the PMD-induced depolarization, provided that PMD itself is fully compensated by DSP in the coherent receiver. With no or small PMD in the fibers, the full transmission spectrum should be taken into account for the performance evaluation. However, with large PMD (>0.1 ps/$\mathrm{km}^{1/2}$), the nonlinear penalty is only weakly dependent on the number of copropagating channels. In addition, we have shown that PMD can still bring some benefit for interleaved RZ-CP-QPSK transmitted in the nonlinear regime despite the fact that PMD breaks out the perfect time alignment for interleaving.

References

[1] C. R. S. Fludger *et al.*, "Coherent equalization and POLMUX-RZ-DQPSK for robust 100-GE transmission," *J. Lightwave Technol.*, vol. 26, no. 1, pp. 64–72, Jan. 1, 2008.

[2] A. Bononi, P. Serena, N. Rossi, and D. Sperti, "Which is the dominant nonlinearity in long-haul PDM-QPSK coherent transmissions?," presented at the Eur. Conf. Opt. Commun., Turin, Italy, 2010, Paper Th.10.E.1.

[3] C. Xie, "Interchannel nonlinearities in coherent polarization division-multiplexed quadrature-phase-shift-keying systems," *IEEE Photon. Technol. Lett.*, vol. 21, no. 5, pp. 274–276, Mar. 1, 2009.

[4] J. Renaudier *et al.*, "Performance comparison of 40G and 100G coherent PDM-QPSK for upgrading dispersion managed legacy systems," presented at the Opt. Fiber Commun. Conf. Exposition, Nat. Fiber Optic Eng. Conf., San Diego, CA, 2009, Paper NWD5.

[5] J. Renaudier *et al.*, "Investigation on WDM nonlinear impairments arising from the insertion of 100-Gb/s coherent PDM-QPSK over legacy optical networks," *IEEE Photon. Technol. Lett.*, vol. 21, no. 24, pp. 1816–1818, Dec. 15, 2009.

[6] M. Winter, C.-A. Bunge, D. Setti, and K. Petermann, "A statistical treatment of cross-polarization modulation in DWDM systems," *J. Lightwave Technol.*, vol. 27, no. 17, pp. 3739–3751, Sep. 1, 2009.

[7] O. Bertran-Pardo *et al.*, "Demonstration of the benefits brought by PMD in polarization-multiplexed systems," presented at the Eur. Conf. Opt. Commun., Turin, Italy, 2010, Paper Th.10.E.4.

[8] P. Serena, N. Rossi, and A. Bononi, "Nonlinear penalty reduction induced by PMD in 112 Gbit/s WDM PDM-QPSK coherent systems," presented at the Eur. Conf. Opt. Commun., Vienna, Austria, 2009, Paper 10.4.3.

[9] C. Xia, J. F. Pina, A. Striegler, and D. van den Borne, "PMD-induced nonlinear penalty reduction in coherent polarization-multiplexed QPSK transmission," presented at the Eur. Conf. Opt. Commun., Turin, Italy, 2010, Paper Th.10.E.5.

[10] S. Pachnicke, A. Chachaj, M. Helf, and P. M. Krummrich, "Fast parallel simulation of fiber optical communication systems accelerated by a graphics processing unit," presented at the Int. Conf. Transparent Opt. Netw., Munich, Germany, 2010, Paper Th.B1.5.

[11] C. Xia and D. van den Borne, "Impact of the channel count on the nonlinear tolerance in coherently-detected POLMUX-QPSK modulation," presented at the Opt. Fiber Commun. Conf. Exposition, Nat. Fiber Optic Eng. Conf., Los Angeles, CA, 2011, Paper OWO1.

[12] G. V. de Faria, M. R. Jimenez, and J. P. von der Weid, "PMD variations from factory to field in OPGW cabled fibers," *IEEE Photon. Technol. Lett.*, vol. 18, no. 1, pp. 250–253, Jan. 1, 2006.

[13] S. Abrate, C. Lezzi, V. Ferrero, A. Nespola, and P. Poggiolini, "Long-term PMD measurements in a metropolitan operational G.652 cable plant," in *Proc. Eur. Conf. Opt. Commun.*, Turin, Italy, 2005, vol. 3, pp. 671–672.

Author biographies not included at author request due to space constraints.